Configuration dependence in calculations for pion inelastic scattering near $N=28$

David S. Oakley*

University of Texas, Austin, Texas 78712
and University of Colorado, Boulder, Colorado 80309

H. T. Fortune

University of Pennsylvania, Philadelphia, Pennsylvania 19104
(Received 6 July 1987)

A recent publication presented angular distributions for 180-MeV pion inelastic scattering for several $N \sim 28$ nuclei. Proton $E2$ matrix elements extracted from those data for certain states were systematically larger than those inferred from γ decay. A possible explanation for these anomalies is discussed.

A recent paper[1] presented values for neutron and proton matrix elements, M_n and M_p, for the nuclei ^{48,50}Ti, ^{52}Cr, and ^{54,56}Fe extracted from a collective-model analysis of pion inelastic scattering data. Agreement between $M_p(\pi)$ and previous electromagnetic measurements, M_p(EM), was good in many cases but not so good in others, as shown in Fig. 1. Here it is noted that the proton strengths determined from pion scattering are in good agreement with previous measurements for states with large $B(E2)$ values, i.e., $B(E2) \geq 1$ W.u. For states seen to be weak in γ decay (states with noncollective $E2$ values to the ground state) however, the strengths from pion scattering are systematically larger (Table I and Fig. 1).[1,2] Values of M_p obtained from neutron, proton, and possibly electron scattering, can be similar to those found from pion scattering (Table II), perhaps indicating the model dependence of the calculations.[3-8] If the $B(E2)$ values are small, a collective-model analysis is certainly suspect and so we have reanalyzed the data for these states using microscopic (single-particle type) transition densities.

Microscopic calculations were performed using the distorted-wave impulse-approximation (DWIA) code DWPI.[1,9] This code was modified to include coordinate-space densities for single-particle transitions from the $1f_{7/2}$ shell to the $1f_{7/2}$ shell, ρ_{ff}, and to the $2p_{3/2}$ shell, ρ_{fp}. Here the ff and fp transition densities have the form[6]

$$\rho_{ff} = \frac{-32}{21\sqrt{21}\pi} b_f^{-9} r^6 \exp[-(r/b_f)^2]$$

and

$$\rho_{fp} = \frac{8\sqrt{2}}{7\pi} b_f^{-9/2} b_p^{-5/2} r^4 \left[1 - \frac{2r^2}{b_p^2} \right]$$

$$\times \exp{-[r^2(b_p^{-2} + b_f^{-2})/2]} ,$$

where the parameters b_f and b_p are determined from electron scattering to be 1.90 and 2.37 fm, respectively,

for the 2^+ states for nuclei in this region.[6]

Collective-model calculations are those from Ref. 1 in which the code DWPI was also used. Those transition densities are given by

$$\rho_{\text{tr}}(r) \sim \beta \frac{d\rho(r)}{dr} ,$$

where ρ is the ground-state density. In both the collective and shell model calculations the neutron density parameters were taken from the previous work.[1]
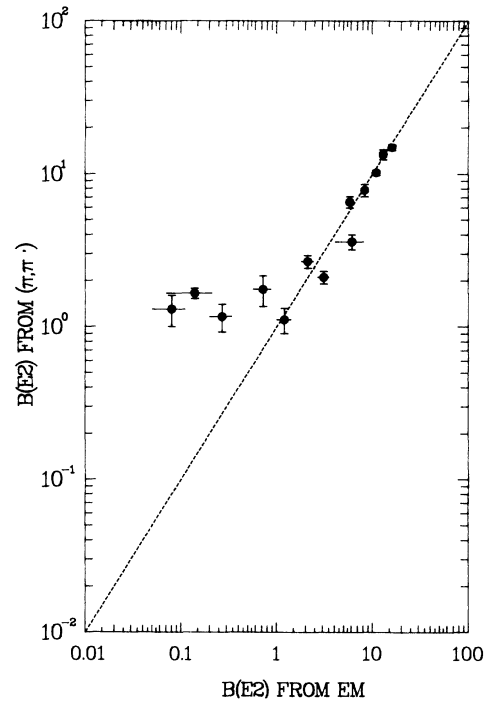

FIG. 1. Plot of $B(E2)$ strengths (in Weisskopf single-particle units, W.u.) from pion scattering (Refs. 1 and 10) versus those from γ decay (Ref. 2). The dashed line results if the two measurements are equal.

TABLE I. Comparison of proton transition strengths (Weisskopf units) from pion scattering and γ decay experiments.

Nucleus	State (J^π)	E_x (MeV)	$B(E2)$ (EM)[a]	$B(E2)$ (π,π')[b]	$B(E2)$ (Present work)[c]
^{48}Ti	2_1^+	0.98	13(1)	13(1)	
	2_2^+	2.42	1.2(0.2)	1.1(0.2)	
^{52}Cr	2_1^+	1.43	11(1)	10(1)	
	2_4^+	3.77	0.14(0.07)	1.7(0.1)	0.14(0.01)
^{54}Fe	2_1^+	1.41	8.3(0.2)	7.8(0.7)	
	2_2^+	2.96	2.1(0.3)	2.7(0.3)	
	2_3^+	3.17	0.72(0.2)	1.8(0.4)	0.72(0.16)
^{56}Fe	2_1^+	0.85	16(1)	15(1)	
	2_2^+	2.66	0.27(0.07)	1.2(0.2)	0.29(0.05)
	2_4^+	3.37	0.08(0.03)	1.3(0.3)	0.09(0.02)

[a]Values are from compilations, Ref. 2.
[b]Values are from collective-model analysis of (π,π'), Ref. 1.
[c]Values are from microscopic (π,π') calculations, this work.

The matrix elements were extracted by simultaneous fits to both the π^+ and π^- data, where the π^+ scatter predominantly from the protons while the π^- scattering affects mostly the neutrons. The form for the matrix element is given by

$$M_i \equiv C\epsilon \int_0^\infty r^{l+2}\rho_{\mathrm{tr},i}(r)dr \quad (i=\mathrm{p,n}) ,$$

where $C = Z$ or N (i=p or n) for collective transitions and unity for microscopic calculations. For even-A nuclei, the $B(E2)$ for an upward transition is simply the

TABLE II. Comparison of $0^+ \rightarrow 2^+$ proton transition strengths (e^2 fm^4) from different experiments.

Nucleus	State (J^π)	E_x (MeV)	$B(E2\uparrow)$ (π,π')[a]	$B(E2\uparrow)$ (EM)[b]	$B(E2\uparrow)$ (p,p')[d]	$B(E2\uparrow)$ (n,n')[e]	$B(E2\uparrow)$ (e,e')[f]
^{48}Ti	2_1^+	0.98	694(52)	673(52)			537(15)
	2_2^+	2.42	58(10)	62(10)			
	2_3^+	3.37	67(16)	73(26)[c]			
^{52}Cr	2_1^+	1.43	589(23)	635(58)	620(125)		632(40)
	2_2^+	2.96		1.2(0.6)	6.7(0.4)		
	2_3^+	3.17		12(4)	77(5)		16(1)
	2_4^+	3.77	95(8)	8(4)	82(6)		112(8)
^{54}Fe	2_1^+	1.41	473(42)	503(12)		296(79)	
	2_2^+	2.96	164(18)	127(18)	300(15)	190(94)	
	2_3^+	3.17	109(24)	44(9)	72(5)	33(13)	
	2_4^+	4.58	47(13)		36(2)		
^{56}Fe	2_1^+	0.85	948(38)	1018(64)		861(389)	945(45)
	2_2^+	2.66	76(13)	17(5)		47(16)	
	2_4^+	3.37	83(19)	5(2)		47(16)	

[a]Values are from (π,π'), Ref. 1.
[b]Values are from compilations, Ref. 2, unless otherwise noted.
[c]Values are from $(\alpha,p\gamma)$, Ref. 8.
[d]Values inferred from (p,p'), Refs. 3 and 4 unless otherwise noted.
[e]Values inferred from (n,n'), Ref. 5.
[f]Values are from (e,e'), Refs. 6 and 7. Errors inferred.

TABLE III. Relative ff- and fp-shell proton contributions to 2^+ states analyzed in this paper.

Nucleus	State (J^π)	E_x (MeV)	α_{ff}	$\alpha_{fp,p}$	$\alpha_{fp,n}$
^{52}Cr	2_4^+	3.77	-0.617	0.686	0.700
^{54}Fe	2_3^+	3.17	-0.195	0.650	0.336
^{56}Fe	2_2^+	2.66	-0.117	0.416	0.630
^{56}Fe	2_4^+	3.37	-0.546	0.598	0.510

square of this matrix element for protons.

It was observed that calculations for pure $f_{7/2} \rightarrow f_{7/2}$ or pure $f_{7/2} \rightarrow 2p_{3/2}$ proton transitions could not simultaneously produce large π^+ cross sections and small $B(E2)$ strengths. For these noncollective states, therefore, we have chosen to analyze the data by using a linear combination of ff and fp transition densities

$$\rho_{tr,p} = \alpha_{ff,p}\rho_{ff} + \alpha_{fp,p}\rho_{fp}$$

and

$$\rho_{tr,n} = \tfrac{1}{3}\alpha_{ff,p}\rho_{ff} + \alpha_{fp,n}\rho_{fp} ,$$

assuming an effective charge ratio of $e_p/e_n = 3.0$ [in both π scattering and $B(E2)$ calculations] and with no direct neutron $f \rightarrow f$ transitions.

In this analysis, we attempt to find the values of the constants α_{fx} that simultaneously give the best fit to the pion data while reproducing the observed $B(E2)$ values from γ decay. These values are listed in Table III with the transition densities shown in Fig. 2. The resulting π^+ angular distributions are compared to the data in Fig. 3. Because the proton transition densities are primarily determined from π^+ scattering, these results are not significantly changed by different choices of effective charge ratios.

While the collective calculations still seem to give a slightly better fit to the angular-distribution shapes, both models are adequate in that regard. However, by extend-
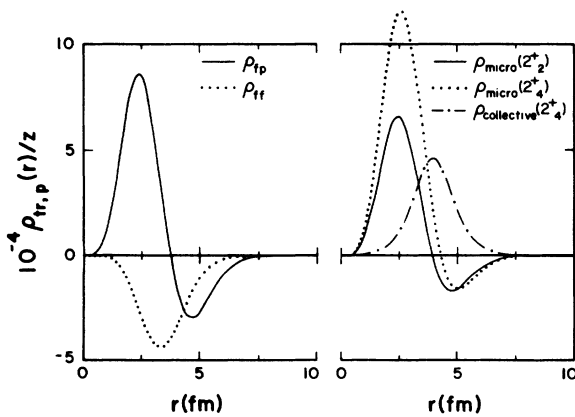

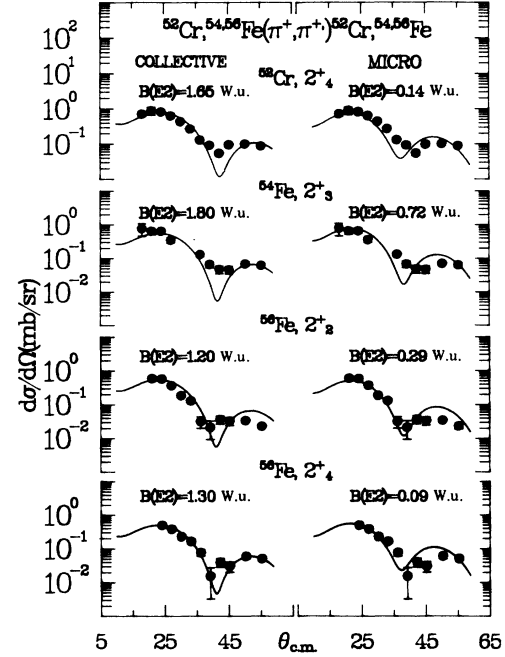FIG. 2. Transition densities used for the microscopic and collective-model ^{56}Fe calculations.

FIG. 3. Inelastic-scattering angular distributions compared with $l=2$ collective-model and $l=2$ microscopic DWPI calculations. The relative microscopic transition densities are as given in Table III.

ing the form factor and thus lowering the strength needed to fit the data, we have been able to reproduce the observed $E2$ strengths with microscopic calculations.

When we extract the neutron matrix elements for this model we find the ratios of M_n/M_p to be different from those extracted in the collective-model calculations (Table IV). This is to be expected for such a microscopic transition density with a large interior component. In this case the pion cross sections calculated for different linear combinations of ρ_{ff} and ρ_{fp} will not change in the same manner as M_n and M_p because these matrix elements result from integrations over the entire volume, whereas π scattering mostly just samples the surface.

TABLE IV. Comparison of ratios of neutron and proton $E2$ matrix elements from microscopic and collective-model analysis of (π,π').

Nucleus	State (J^π)	E_x (MeV)	M_n/M_p [a]	M_n/M_p [b]
^{52}Cr	2_4^+	3.77	1.46(0.14)	2.53(0.24)
^{54}Fe	2_3^+	3.17	0.78(0.12)	0.57(0.09)
^{56}Fe	2_2^+	2.66	1.53(0.14)	1.84(0.17)
^{56}Fe	2_4^+	3.37	1.11(0.14)	2.05(0.26)

[a]Collective-model values, from Ref. 1.
[b]Microscopic values, from this work.

To conclude, we have exhibited microscopic transition densities that both describe the pion-scattering data and reproduce the $E2$ strengths from γ-decay measurements. From this we see that the ratio M_n/M_p appears to be very model dependent just as does the absolute electromagnetic strength. The question of whether these microscopic amplitudes are realistic or not awaits confirmation by a sophisticated shell-model calculation.

*Present address: University of Colorado, Boulder, CO 80309.

[1]D. S. Oakley et al., Phys. Rev. C 35, 1392 (1987).

[2]P. M. Endt, At. Data Nucl. Data Tables 23, 547 (1979).

[3]B. M. Preedom et al., Phys. Rev. C 2, 166 (1970).

[4]M. Fujiwara et al., Phys. Rev. C 32, 830 (1985).

[5]S. Mellema, R. W. Finlay, and F. S. Dietrich, Phys. Rev. C 33, 481 (1986).

[6]J. W. Lightbody et al., Phys. Rev. C 27, 113 (1983).

[7]B. J. Linard et al., Nucl. Phys. A302, 214 (1978).

[8]J. Heisenberg, J. S. McCarthy, and I. Sick, Nucl. Phys. A164, 353 (1971).

[9]R. A. Eisenstein and G. A. Miller, Comput. Phys. Commun. 11, 95 (1976).

[10]K. G. Boyer et al., Phys. Rev. C 24, 598 (1981).